

Optimization of Heat Transfer Area for Multiple Effects Desalination (MED) Process

Salih M. Alsadaie^a, Sana I. Abukanisha^a, Amhamed A. Omar^b, and Iqbal M. Mujtaba^{c*}

^a Sirte University, Department of Chemical Engineering, Sirte, Libya

^b Sirte Oil Company, National Oil Corporation, Libya

^c Bradford University, Department of Chemical Engineering, Bradford BD7 1DP, UK

* Corresponding Author: I.M.Mujtaba@bradford.ac.uk.

ABSTRACT

Seawater desalination is considered as the only available solution that can cope with the increasing demand for freshwater around the world. Improving the desalination techniques may help to cut off the cost and increase sustainability. In this paper, a mathematical model describing the MED process is developed within gPROMs software. The model includes all the necessary mass and energy balance equations together with thermodynamic and physical properties equations. The model predictions are validated against the actual plant data before using the model for optimizing the process to achieve minimum heat transfer area. For two different operating conditions (summer and winter) and a fixed production demand, the heat transfer area is minimised while optimising different parameters of the MED process. The results showed that a 10.4% reduction in the heat transfer area can be achieved under summer operating conditions and around 26% decrease in the heat transfer area can be met under winter operating conditions.

Keywords: gProms, Modelling and Simulations, Optimization, MED Desalination, Heat Transfer Area

INTRODUCTION

The improvement in the living standard and increasing abstraction of available freshwater put more stress on the desalination industries to cope with the increasing demand for freshwater. Unfortunately, seawater desalination is the last and maybe the only available option to produce freshwater by removing the salt from the seawater. However, with the increasing world population and improved standard of living, freshwater production processes face the challenge of producing freshwater at higher quality and lower cost. The most known techniques for water desalination are thermal techniques such as Multistage Flash desalination (MSF) and Multiple Effect desalination (MED) and membrane techniques such as Reverse Osmosis (RO). Although the installed capacity of (RO) remarkably surpasses the MSF and MED [1], the MED process, operating considerably at a much lower temperature, is more preferred option for new construction plants in different locations around the world where waste heat is available [2]. However, the MED desalination technology is highly energy intensive (ranging from 5.5 to 20 kW h/m³) [3]. In addition, the product cost

of freshwater from the MED process may vary between 0.27 and 1.49 USD/m³ [4]. It is still quite expensive and hence, it is believed that more work is required to cut off the costs and increase the profitability by operating the plant at minimal energy consumption. Some previous studies in the literature have been carried out to reduce the cost of freshwater by hybrid MED process with other desalination techniques. Al-hotmani et al. [5] integrated the MED process with the RO process to find more room for improvement. With a slight reduction of the consumed energy, the results showed that 9% increase in production rate and a 5% reduction in the brine flow rate. Others attempt to reduce the cost by powering the MED process with renewable sources of energy such as wind and solar energy. Kaabinejadian et al. [6] investigated the advantages of integration of MED with a humidification-dehumidification (HDH) unit powered by solar energy. The optimised total cost is found to be 0.548 \$/s. Moreover, integrating the HDH unit with the MED process resulted in an increase in the freshwater production and the cost by 0.5% and 0.1%, respectively. However, the main drawbacks of renewable energies are their dependencies on climate conditions (available sunshine, wind power). The

optimization of a single MED process can be classified into two categories; finding the optimal operating conditions that result in minimum energy consumption and maximum production rate and/or finding the optimum design configuration that results in minimum fixed cost of the plant. Al-Mutaz and Wazeer [7] optimized the number of effects that result in minimum capital cost and steam cost. The results showed that increasing the number of effects from 11 to 15 would result in a reduction of water cost by 0.029 \$/m³. With the aid of solar energy as supplied heat, Talebbeydokhti, et al. [8] carried out a performance analysis to investigate the feasibility of finding the optimum operating conditions at different numbers of effects and different heat sources. Processes with different number of effects (7, 9 and 11 effects) were investigated and obtained optimum operating conditions for each case. Sadri et al. [9] conducted multi-objective optimization to increase the gain output ratio (GOR) and minimise the heat transfer area. For the fixed mass flow rate of the seawater, the results showed an increase of 11.32 % in the GOR and a 17.29 % reduction in the heat transfer area. Harandi et al. [10] performed multi-objective optimization for the MED process integrated with a gas power plant using nondominated sorting genetic algorithm II. Considering GOR and annual cost as objective functions, it was found that higher GOR can be obtained for 9 effects MED and lower annual cost can be obtained for 4 effects MED. Rivera et al. [11] carried out multi-objective optimization for two different-sized MED plants one with 9 effects and the second with 12 effects. The objective of the study was to find optimum operating conditions that minimise the thermal energy and the cost of produced water and maximize the production rate. The authors claimed that different optimal solutions can be found depending on the objectives of the optimization.

Most of the previous studies consider the MED process in one single mode (Summer/Winter) and a typical MED configuration. In this paper, a mathematical model for MED is developed and solved using gPROMs software. For a fixed production rate, several operating parameters are optimized to minimise the heat transfer area of the MED process. Unlike most of the previous works, the optimization procedure is conducted for two different seasons (summer and winter). Further, the MED plant under investigation interestingly has a different design configuration with two large effects and two small effects combined together in a single MED process which makes it unique to other types of MED plants around the world.

MED PROCESS DESCRIPTION

The MED process, as presented in Figure 1, consists of two large effects, two small effects and a condenser. The heating steam coming from the ejector flows inside the tubes of the first effect while a portion of the feed

seawater is sprayed around the outside surface of the tubes of the first effect. The other seawater portion is divided over the rest of the effect based on the size of each effect. The release of the latent heat of the steam causes an increase in the temperature of the seawater resulting in the evaporation of some water. The evaporated water then flows through the channel into the tubes of the second effect and the process is repeated until the fourth effect. In most configurations of the MED, part of the low-pressure entrained vapour is taken from the last effect and introduced to high-pressure motive steam through the ejector. However, in the MED process considered here, the part of the low-pressure-entrained vapour is taken from the second effect leading to a smaller amount of vapour entering the third and fourth effects. As a result, the installed third and the fourth effects have a smaller area. More details of the process can be found in the literature.

MATHEMATICAL MODEL OF MED PROCESS

A steady-state mathematical model is developed to simulate the MED process. The model is built based on mass and energy balance equations, and it is supported with physical and thermodynamic properties correlations. The developed model is divided into three parts: evaporators, a steam ejector and a down condenser. The two plate heat exchangers are also modelled as a simple heat exchanger, but their model equations are not included here. More details of the model equations and physical properties correlations can be obtained from Al-Mutaz and Wazeer [12]. For the sake of simplicity and to obtain reasonable results from the model, the following assumptions are made:

1. The distillate product is salt-free.
2. There are no heat losses to the surroundings as the equipment is well insulated.
3. The release of non-condensable gases is neglected.
4. The heat of mixing is neglected.

The following are the governing equations of the process including the physical properties correlations.

Evaporator

$$\Delta T = [T_{b_out(1)} - T_{b_out(n)}] / [n - 1] \quad (1)$$

$$T_{b_out(1)} = T_s - \Delta T \quad (2)$$

$$T_{b_out} = T_{b_in} - \Delta T \quad (3)$$

$$T_{v_out(1)} = T_{b_out(1)} - BPE \quad (4)$$

$$F + B_{in} = V_{vapour} + V_{brine} + V_{dist} + B_{out} \quad (5)$$

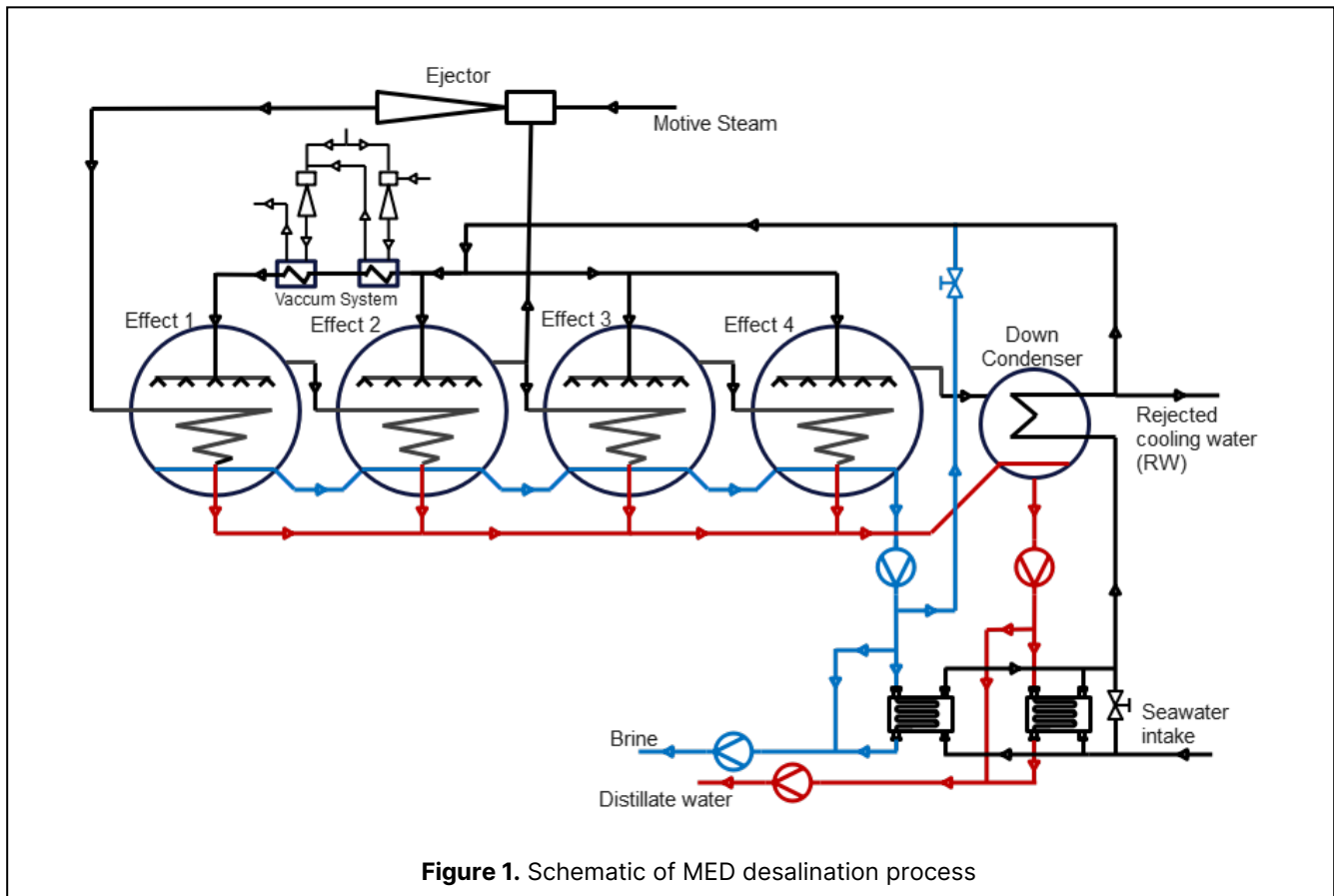


Figure 1. Schematic of MED desalination process

$$X_F F + X_{b_in} B_{in} = X_{b_out} B_{out} \quad (6)$$

$$V_{in} \lambda_{in} = F C p_w (T_{b_out} - T_f) + V_{vapour} \lambda_{out} \quad (7)$$

$$V_{in} \lambda_{in} = A_e U (T_{v_in} - T_{v_out}) \quad (8)$$

$$V_{brine} = [B_{in} C p_{brine} (T_{b_{in}} - T')]/[\lambda_{in}] \quad (9)$$

$$T' = T_{b_out} - NEA \quad (10)$$

$$NEA = [33(T_{b_{in}} - T_{b_out})^{0.55}]/[T_{v_out}] \quad (11)$$

$$V_{dist} = [D_{in} C p_{dist} (T_{cond} - T')]/[\lambda_{out}] \quad (12)$$

$$T'' = T_{v_out} + NEA' \quad (13)$$

$$NEA' = [33(T_{C_{in}} - T_{v_out})^{0.55}]/[T_{v_out}] \quad (14)$$

$$T_{cond} = T_{v_in} - \Delta T_{loses} \quad (15)$$

$$V_{out} = V_{vapor} + V_{brine} + V_{dist} \quad (16)$$

Down Condenser

$$V_{out(n)} \lambda_{out(n)} = F C p_{cw} (T_f - T_{cw}) \quad (17)$$

$$V_{out(n)} \lambda_{out(n)} = A_c U_c LMTD_C \quad (18)$$

$$LMTD_C = [(T_f - T_{cw})]/\left[\ln\left(\frac{T_{v_out} - T_{cw}}{T_{v_out} - T_f}\right)\right] \quad (19)$$

Steam Injector

$$M_s = M_{ev} + M_u \quad (20)$$

$$R_a = 0.296 \frac{P_s^{1.19}}{P_{ev}^{1.04}} \left(\frac{P_m}{P_{ev}}\right)^{0.015} \left(\frac{PCF}{TCF}\right) \quad (21)$$

$$PCF = 3 \times 10^{-7} (P_m^2) - 0.0009 P_m + 1.6101 \quad (22)$$

$$TCF = 2 \times 10^{-8} (T_{ev}^2) - 0.0009 T_{ev} + 1.0047 \quad (23)$$

$$CR = P_s/P_{ev} \quad (24)$$

$$P_s = 1000 \times \exp\left(\frac{-3892.7}{T_s + 273.15 - 42.6776} + 9.5\right) \quad (25)$$

$$P_{ev} = 1000 \times \exp\left(\frac{-3892.7}{T_{ev} + 273.15 - 42.6776} + 9.5\right) \quad (26)$$

$$GOR = D_{total}/M_s \quad (27)$$

Physical properties correlations

Specific Heat Capacity (Cp)

$$C_p = (a + bT + cT^2 + dT^3) \times 10^{-3}$$

Where:

$$a = 4206.8 - 6.6197 S + 1.2288 \times 10^{-2} S^2$$

$$b = -1.1262 + 5.4178 \times 10^{-2} S - 2.2719 \times 10^{-4} S^2$$

$$c = 1.2026 \times 10^{-2} - 5.3566 \times 10^{-4} S - 1.8906 \times 10^{-6} S^2$$

$$d = 6.877 \times 10^{-7} + 10517 \times 10^{-6} S - 404268 \times 10^{-9} S^2$$

Boiling Point Elevation

$$BPE = X_b \times ((A + B \times X_b) + (C \times X_b^2))$$

$$A = 8.325 \times 10^{-2} + 1.883 \times 10^{-4} T_{b-out} + 4.02 \times 10^{-6} T_{b-out}^2$$

$$B = -7.625 \times 10^{-4} + 9.02 \times 10^{-5} T_{b-out} - 5.02 \times 10^{-7} T_{b-out}^2$$

$$C = 1.522 \times 10^{-4} - 3 \times 10^{-6} T_{b-out} - 3 \times 10^{-8} (T_{b-out})^2$$

Boiling Point Elevation

$$\lambda_{in} = 2499.5689 - 2.20486 T_s - 0.00176 T_s^2$$

$$\lambda_{out} = 2499.5689 - 2.20486 T_{v-out} - 0.00176 T_{v-out}^2$$

In the above two equations, the temperature is in °C, and latent heat is in kJ/kg.

Simulation and Validation

The MED plant under this investigation is located in Sirte, Libya. It was installed in 2010 and got into actual operation after 2016. Table 1 presents input operating parameters for two different modes: summer mode and winter mode. The accuracy of the model predictions is very important in any simulation. Hence, the model is validated against actual data for the summer mode. The actual plant data and the simulation results are shown in Table 2. As can be seen, good agreement against actual data has been obtained. Normally in winter mode, the plant operates in different conditions. However, due to the lack of full actual winter operating data from the plant, the validation is carried out only against summer operating data.

Table 1: Input parameters of 4 effects MED process for summer and winter modes

Parameters	Summer mode	Winter mode
Motive steam pressure (bar)	11.4	11.4
Motive steam flowrate (kg/s)	5.85	5.85
Inlet steam temperature to the first effect (°C)	68.5	68.5
Mass flow of the seawater to the effects (kg/s)	144.44	144.44
Intake seawater temperature (°C)	27	14
Recycle brine flowrate (kg/s)	0.0	60.444
Last stage brine outlet temperature (°C)	52	50

Optimization Problem

To obtain the optimal operating conditions that result in a minimum heat transfer area, an optimization approach is carried out to minimize the heat transfer area at a fixed demand of freshwater. Motive steam flowrate, entrained vapour to the ejector, last effect's brine tempera-

ture, feed flowrate and intake seawater flowrate are optimized to achieve the objective. For winter mode, the recycle brine flow rate is also optimized. To maintain the feasible operating conditions, the optimised parameters are controlled by introducing equality and inequality constraints including lower and upper desalination plant limits.

Table 2: Validation of the simulation results against actual operating parameters.

Parameters	Values		
	Actual	Model	Error
Top Boiling Temp. (°C)	64	64.38	0.6%
Distillate flowrate (kg/s)	47.91	45.89	-4.2%
Distillate water temp. (°C)	52	51.45	-1%
The feed seawater temp. (°C)	46.41	46.72	0.7%
Heat transfer area, Ae (m ²)			
First effect	3760	3674.2	-2.3%
Second effect	3760	3673.2	-2.3%
Third effect	810	775.8	-4.2%
Fourth effect	810	779.6	-3.7%
Gain Output Ratio (GOR)	8.19	7.82	-4.5%

The optimization problem can be described as follows:

Optimization Problem

Minimize

Optimize

Ae

Mev, Mu, Tb(n), F, seawater intake and brine recycle for winter mode only

Subject to:

Equality constraints: the fixed demand for freshwater ($D_{TOTAL} = 45.89$ kg/s)

Inequality constraints: the lower and upper limits of some constraints are different between summer and winter.

Table 2

Summer conditions			Winter conditions		
Lower	Parameter	upper	Lower	Parameter	upper
0.0	< RW (kg/s)	< 50	0.0	< RW (kg/s)	< 50
1.0	< CR	< 3.0	1.0	< CR	< 3.0
44	< Tf (°C)	< 50	40	< Tf (°C)	< 50
35	< Td* (°C)	< 45	25	< Td* (°C)	< 35
35	< Tb** (°C)	< 45	25	< Tb** (°C)	< 35

* Temperature of the distillate leaving the distillate plate heat exchanger

** Temperature of the brine leaving the brine plate heat exchanger

Table 3 shows the new values of the optimized parameters for summer and winter conditions. The flow rate of the main source of energy which is the motive steam slightly decreased by 1.5 % in summer and increased by 3.6 % in winter. In addition, table 4 depicts the results of the optimization process. As can be seen, the values of the constraints in the optimization problem did not violate the constraints' limits. Table 5 shows the results of the optimization process. Interestingly, the total heat transfer area for the 4 effects has been reduced by 10.4% in summer and by 26% in winter. Hence, the new design of the MED process should be based on summer conditions which require more available area. If the MED process is designed based on winter conditions, the available area can not meet the demand for freshwater in the summer season. Other parameters are in the feasible values and the MED process can operate at the new conditions comfortably.

Table 3: Optimized parameters and the optimization results for the two seasons

Optimized parameters		
Parameters	Summer	Winter
Motive steam flowrate, (kg/s)	5.76	6.06
Entrained vapour flowrate, kg/s	13.68	10.97
Last effect temperature °C	49.67	43.0
Feed flowrate, kg/s	150.95	170
Seawater intake flowrate, kg/s	170	135
Brine recycle flowrate, kg/s	-	40.32

Table 4: optimization results for the two seasons.

Optimization results		
Parameters	Summer	Winter
Rejected water (RW) (kg/s)	19.04	6.01
CR	1.569	1.83
Tf (°C)	44.75	46.67
Td* (°C)	35.2	25.14
Tb** (°C)	36.1	26.09

Table 5: Objective function of the optimization process.

Summer	Winter
1 st effect = 3426.2 m ²	1 st effect = 2338.1 m ²
2 nd effect = 3343.7 m ²	2 nd effect = 2230.1 m ²
3 rd effect = 589.10 m ²	3 rd effect = 638.60 m ²
4 th effect = 620.20 m ²	4 th effect = 732.10 m ²
Total area = 7979.2 m ²	Total area = 5938.9 m ²

Total area reduction is 10.4% in summer mode and 26% in winter mode.

CONCLUSIONS

The optimization problem to minimize the heat

transfer area has been solved and the minimum required heat transfer area has been achieved. To accomplish this goal, a detailed mathematical model for the MED process was developed and validated against actual plant data. For a fixed freshwater demand, the results showed the possibility of designing the MED process with less heat transfer area. Moreover, the results depicted that the MED process should be designed based on the summer conditions due to a higher available area and lower motive steam. Moreover, the demand for the freshwater is higher in the summer than in the winter.

NOMENCLATURE

Ac	Heat transfer area of the condenser (m ²)
Ae	Heat transfer area of the effect (m ²)
Bin	Brine flow rate entering the effect (kg/s)
Bout	Brine flow rate leaving the effect (kg/s)
BPE	Boiling Point Elevation (°C)
Cpbrine	Heat capacity of the brine (kJ/kg.°C)
Cpdist	Heat capacity of the distillate (kJ/kg.°C)
Cpw	Heat capacity of seawater (kJ/kg.°C)
CR	Pressure ratio of compressed steam and entrained steam.
Din	Distillate flow rate entering the flash box (kg/s)
DTotal	Total product flowrate (kg/s)
F	Seawater feed flow rate to the effect (kg/s)
GOR	gain output ratio (kg distillate/kg stem)
LMTD	Logarithmic mean temperature difference
Mev	Mass flow rate of the entrained steam (kg/s)
Ms	Mass flow rate of the compressed steam (kg/s)
Mu	Motive steam (kg/s)
n	Number of effects
NEA	Non-Equilibrium Allowance.
PCF	The motive steam pressure correction factor
Pev	Pressures of the entrained steam (kPa)
Pm	Pressures of the motive steam (kPa)
Ps	Pressures of the compressed steam (kPa)
Ra	Mass ratio of motive steam to entrained steam
RW	Rejected cooling water flow rate (kg/s).
T'	Temperature to which the brine cools down as it enters the next effect (°C).
T''	Temperature of the condensing vapour as it enters the flash box (°C)
Tb_in	Brine inlet temperature (°C)
Tb_out	Outlet temperature of brine (°C)
Tc_in	Inlet temperature of the distillate entering the effect (°C)
TCF	The motive steam temperature correction factor
Tcond	The temperature of the distillate vapour (°C)
Tcw	Temperature of intake seawater (°C)
Tf	Temperature of feed seawater (°C)
Ts	Inlet steam temperature (°C)
Tv_in	Inlet temperature of the vapour (°C)
Tv_out	The outlet temperature of the vapour (°C)

U The overall heat transfer coefficient ($\text{Kw/m}^2\cdot^\circ\text{C}$)
 Uc The overall heat transfer coefficient of the condenser ($\text{Kw/m}^2\cdot^\circ\text{C}$)
 V_{brine} Flow rate of the released vapour from the brine pool (kg/s)
 V_{in} Input vapour flow rate (kg/s)
 V_{out} Outlet vapour flow rate (kg/s)
 V_{vapour} Vapour evaporated over the surface of the tubes (kg/s)
 X_b Salinity (ppm)
 X_{b_in} Inlet brine salinity (ppm)
 X_{b_out} Outlet brine salinity (ppm)
 V_{brine} Flow rate of the released vapour from the brine pool (kg/s)
 V_{dist} Flow rate of the released vapour from the distillate pool (kg/s)
 X_f Feed salinity (ppm)

Greek letters

λ_{in} Latent heat of the entering vapour at the inlet vapour temperature ($\text{kJ/kg}\cdot^\circ\text{C}$)
 λ_{out} Latent heat of the released vapour at the outlet vapour temperature ($\text{kJ/kg}\cdot^\circ\text{C}$)
 Δt Temperature difference ($^\circ\text{C}$)

REFERENCES

1. Mayor, B., "Growth patterns in mature desalination technologies and analogies with the energy field," *Desalination*, vol. 457, pp. 75-84, 2019.
2. Prajapati, M., Shah, M., and Soni, B., "A comprehensive review of the geothermal integrated multi-effect distillation (MED) desalination and its advancements," *Groundwater for Sustainable Development*, vol. 19, p. 100808, 2022.
3. Ren, J., Zhao, H., Wang, M., Miao, C., Wu, Y., and Li, Q., "Design and Investigation of a Dynamic Auto-Adjusting Ejector for the MED-TVC Desalination System Driven by Solar Energy," *Entropy*, vol. 24, p. 1815, 2022.
4. Shahouni, R., Abbasi, M., Kord, M., and Akrami, M., "Modelling and optimising of MED-TVC seawater desalination plants assisted with electric heaters," *Water Resources and Industry*, vol. 32, p. 100262, 2024.
5. Al-hotmani, O. M. A., Al-Obaidi, M. A. A., John, Y. M., Patel, R., and Mujtaba, I. M., "An innovative design of an integrated MED-TVC and reverse osmosis system for seawater desalination: process explanation and performance evaluation," *Processes*, vol. 8, p. 607, 2020.
6. Kaabinejadian, A., Moghimi, M., and Fakhari, I., "Design, modeling, and thermo-economic optimization of an innovative continuous solar-powered hybrid desalination plant integrated with latent heat thermal energy storage," *Applied Thermal Engineering*, vol. 219, p. 119576, 2023.
7. Al-Mutaz, I. S. and Wazeer, I., "Economic optimization of the number of effects for the multieffect desalination plant," *Desalination and Water Treatment*, vol. 56, pp. 2269-2275, 2015.
8. Talebbeydokhti, P., Cinocca, A., Cipollone, R., and Morico, B., "Analysis and optimization of LT-MED system powered by an innovative CSP plant," *Desalination*, vol. 413, pp. 223-233, 2017.
9. Sadri, S., Ameri, M., and Khoshkhou, R. H., "Multi-objective optimization of MED-TVC-RO hybrid desalination system based on the irreversibility concept," *Desalination*, vol. 402, pp. 97-108, 2017.
10. Harandi, H. B., Asadi, A., Rahnama, M., Shen, Z.-G., and Sui, P.-C., "Modeling and multi-objective optimization of integrated MED-TVC desalination system and gas power plant for waste heat harvesting," *Computers & Chemical Engineering*, vol. 149, p. 107294, 2021.
11. Rivera, C., Cuevas, C., and Farías, Ó., "Multi-objective optimization with multiple Pareto frontiers applied to a MED desalination system," *Energy Conversion and Management*, vol. 287, p. 117076, 2023.
12. Al-Mutaz, I. S. and Wazeer, I., "Development of a steady-state mathematical model for MEE-TVC desalination plants," *Desalination*, vol. 351, pp. 9-18, 2014.

© 2025 by the authors. Licensed to PSEcommunity.org and PSE Press. This is an open access article under the creative commons CC-BY-SA licensing terms. Credit must be given to creator and adaptations must be shared under the same terms. See <https://creativecommons.org/licenses/by-sa/4.0/>

